Single-crystalline Sb-doped SnO_2 nanowires: synthesis and gas sensor application

Q. Wan*[a] and T. H. Wang[b]

Received (in Cambridge, UK) 22nd March 2005, Accepted 27th May 2005
First published as an Advance Article on the web 23rd June 2005
DOI: 10.1039/b504094a

The synthesis of semiconducting Sb-doped SnO_2 nanowires in mass production by an *in situ* doping approach are reported, and the ethanol sensing results demonstrated that Sb-doped SnO2 nanowires have a promising application for the fabrication of gas sensors with low resistance, and quick response and recovery times.

Semiconducting SnO_2 based films have found a wide range of applications in the fields of transparent conducting electrodes, varistor devices, gas sensors and lithium ion batteries.[1–5] Doping with appropriate elements, such as indium (In) and antimony (Sb), can modulate the optical and electrical properties of SnO_2.[6,7] Addition of these elements would greatly reduce the resistivity of SnO_2 films. For example, Sb-doped SnO_2 thin films with a low electrical resistivity of 9.8×10^{-4} Ω cm have been synthesized by the pulsed-laser deposition method on glass substrates.[6]

Recently, SnO_2 one-dimensional (1D) nanostructures, such as nanobelts, nanowires, and nanorods, have attracted much attention because of their wide applications in nanoscale devices.[8–11] These nanostructures have a large surface-to-volume ratio, which makes them natural contenders as gas sensors. Pure $SnO_2$1D nanostructures could be easily synthesized by many methods, but there is rarely any report on doped 1D SnO_2 nanostructure synthesis and applications because introduction of dopants into the lattice matrices while preserving structural integrity is still a major challenge in metal oxide 1D nanostructure synthesis.[12]

In our previous experiment, undoped SnO_2 nanowires were successfully synthesized by the thermal evaporation method.[13] In this communication, we report the synthesis and gas sensor application of Sb-doped SnO_2 nanowires. We find that Sb doping has a great influence on the electrical properties of the SnO_2 nanowires. Gas sensing results indicated that Sb-doped SnO_2 nanowires showed promise for application in gas sensors with quick response and recovery times.

The thermal evaporation process in the present experiment is similar to that described previously for ZnO nanowire and pure SnO_2 nanowire synthesis.[13,14] High pure (99.99%) metal Sn and Sb powders mixed in the weight ratio of 10 : 1 were used as the evaporation sources. 5 nm gold coated Si wafers (1.0 cm × 1.0 cm) were used as the substrates for sample collection. The temperature at the center of quartz tube is 900 °C, and a constant flow of 1% oxygen and 99% nitrogen was maintained at a rate of 5 l min^{-1}. The morphology of the as-synthesized products was observed by a field emission scanning electron microscope (SEM, JSM-6700F).

As shown in Fig. 1(a), lots of nanowires with a diameter size of 40–100 nm and lengths up to several tens of micrometres were uniformly distributed on the Si substrate. The X-ray diffraction (XRD, D/max 2550 V, Cu Kα radiation) pattern of the synthesized nanowires is presented in Fig. 1(b). All diffraction peaks can be perfectly indexed as the tetragonal rutile SnO_2 structure. The lattice constants of the nanowires calculated from the XRD data are $a = b = 0.474$ nm and $c = 0.319$ nm.

Further insight into the detailed structure of the nanowires was gained by transmission electron microscopy (TEM). A typical TEM image of the as-synthesized nanowires is shown in Fig. 2(a). The image inset in Fig. 2(a) shows a high-resolution image of a single nanowire. Clear lattice fringes in the HRTEM image suggest that each nanowire is a single crystal. In order to check whether Sb was doped into theSnO_2 nanowires, energy-dispersive X-ray spectroscopy (EDS) analysis was performed. As shown in Fig. 2(b), EDS spectra reveal that the synthesized nanowires are composed of Sn, O and Sb. The atomic percentage Sb in the

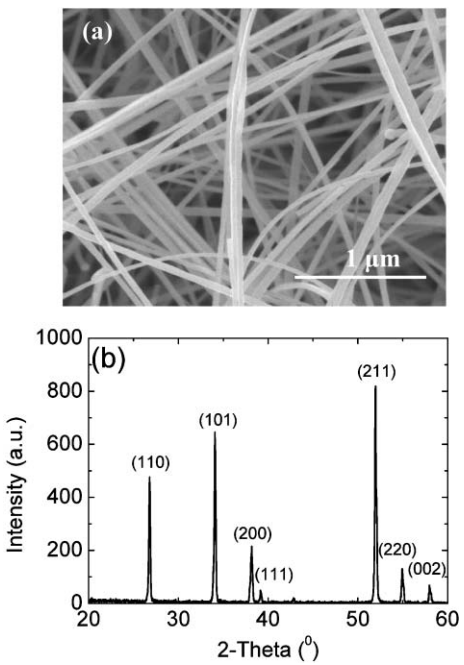

Fig. 1 (a) Emission scanning electron microscope (SEM) image of the synthesized sample, lots of nanowires are observed, (b) X-ray diffraction (XRD) pattern of the synthesized nanowires.

[a]*Department of Materials Science and Metallurgy, The University of Cambridge, Pembroke Street, Cambridge, UK CB2 3QZ. E-mail: qw210@cam.ac.uk; Tel: 44 1223 334357*
[b]*Micro-Nano Technologies Research Center, Hunan University, Changsha 410082, China*

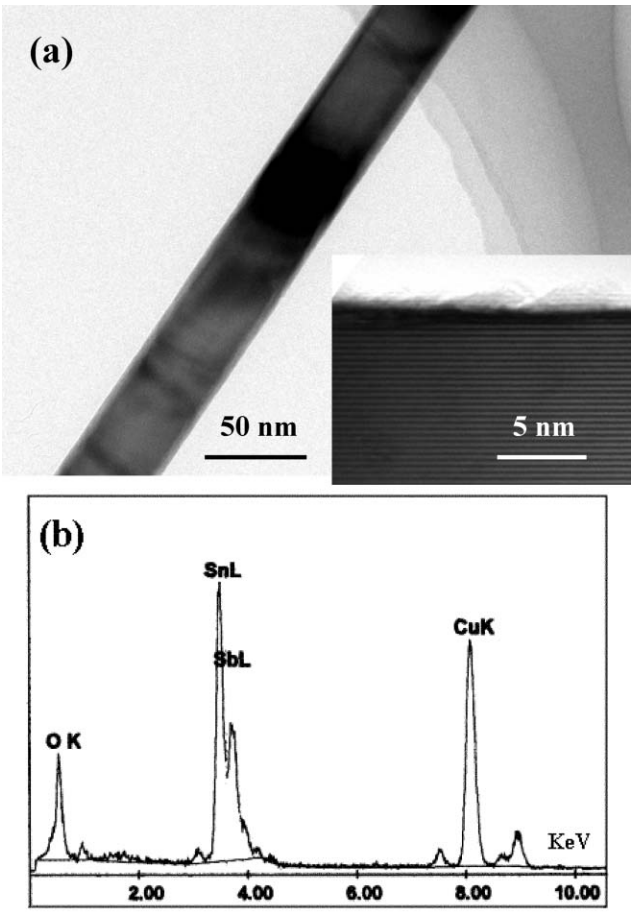

Fig. 2 (a) Transmission electron microscopy (TEM) image of an individual Sb-doped SnO_2 nanowire, inset image shows a high-resolution image of the synthesized nanowires, (b) energy-dispersive X-ray spectroscopy (EDS) of the synthesized nanowires, which reveals that the samples are composed of Sn, O and Sb.

synthesized sample is found to about 3.5 at%. The peaks of Cu come from the Cu grids.

After structural characterizations, undoped and Sb-doped SnO_2 nanowires were ultrasonically dispersed in ethanol. In order to study the influence of Sb doping on the electrical characteristics of SnO_2 nanowires, solutions of two kinds of nanowires with the same concentration were deposited onto the gold (Au) electrodes and annealed at 300 °C in air for 1 h. A schematic picture of the fabricated device is shown in Fig. 3(a). The measured current–voltage curves of both samples are shown in Fig. 3(b). The resistance of the undoped SnO_2 nanowire film was very high because no obvious current was measured. This high resistance is likely to be due to the highly pure stoichiometry of the synthesized SnO_2, which gave a semi-insulating electrical property. After Sb doping, the measured current is about 0.4 mA at a voltage of 10 V, and the resistance is calculated to be about 2.5×10^4 Ω. The resistance decrease is due to the formation of shallow donor levels by introduction of Sb^{+5} into SnO_2,[5] which is very favorable for gas sensor applications.

To further exploit the application of Sb-doped SnO_2 nanowires for gas sensor fabrication, we measured their electrical response and recovery upon exposure to ethanol vapor (concentration:

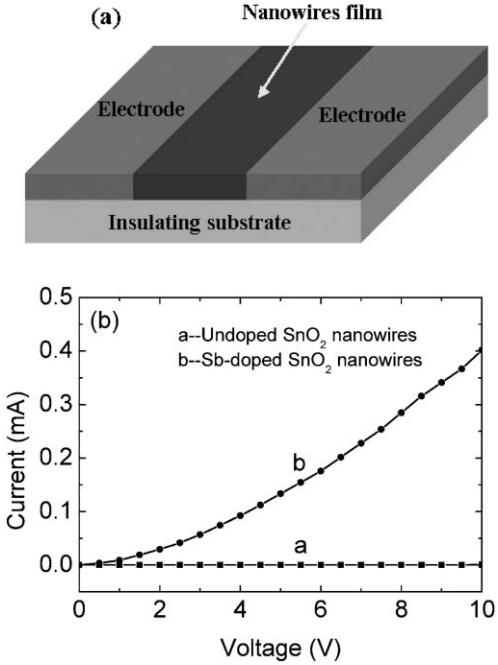

Fig. 3 (a) Schematic illustration of the fabricated device structure for electrical measurement, and (b) the measured current–voltage (*I–V*) curves of both samples.

10–1000 ppm) at a working temperature of 300 °C. As shown in Fig. 4(a), the resistance change of the Sb-doped SnO_2 nanowires is very clear when the atmosphere is changed. The response and recovery times to 10 ppm ethanol are only about 1 s and 5 s, respectively. The resistance of undoped SnO_2 nanowire film is so high that almost no resistance change could be measured with the existing gas sensor test system in our laboratory. In ref. 15, the recovery time of pure SnO_2 nanobelt sensors to ethanol was longer than 10 min. Thus, Sb doping can greatly reduce the recovery time of SnO_2 nanostructured gas sensors to ethanol. It is likely that Sb doping would favor or accelerate the absorption of oxygen molecules and the formation of O_2^- ions on the surface of SnO_2 nanowires, which is of great significance to reduce the recovery times of the fabricated sensor. Further investigations are necessary in order to evaluate the role of Sb doping for the recovery improvement of SnO_2 nanowire sensors.

The gas sensitivity, S_g, is defined as R_a/R_g, where R_a is the electrical resistance in air, and R_g is the resistance in ethanol–air mixed gas. The S_g of the Sb-doped SnO_2 nanowires is 1.76 upon exposure to 10 ppm ethanol. The sensitivity *vs.* ethanol concentration at 300 °C is shown in Fig 4(b). The sensitivity increases with the rising of ethanol gas concentration. In fact, the sensitivity of the semiconducting metal oxide can usually be empirically represented as: $S_g = 1 + P_g^{\beta}$, where P_g is the target gas partial pressure, which is directly proportional to its concentration, and the sensitivity is characterized by the prefactor, P, and exponent, β.[16] β may have some rational fraction value (usually 1 or 1/2), depending on the charge of the surface species and the stoichiometry of the elementary reactions on the surface. In the case of Sb-doped SnO_2 nanowires, β was found to be 1/2 with the ethanol concentration in the range 1–1000 ppm. A theoretical curve of the empirical model of the gas sensitivity was also shown

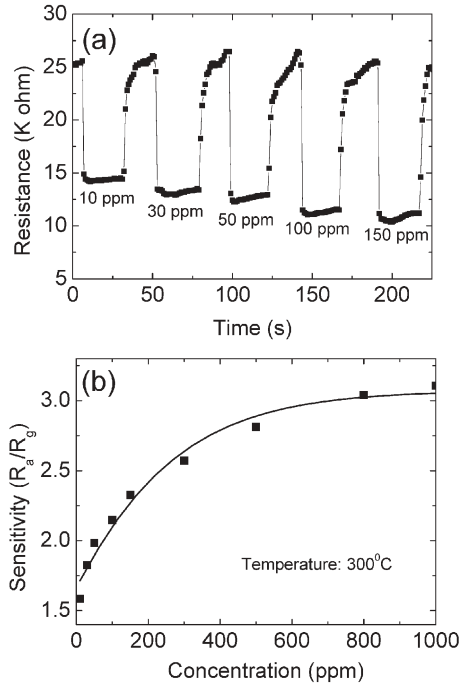

Fig. 4 Five cycles of response–recovery characteristics of Sb-doped nanowires exposed to different ethanol concentrations, and (b) sensitivity *vs.* ethanol concentration in the range of 10–1000 ppm, The solid line is the theoretical curve of the empirical model.

in Fig 4(b). It is found that our measured data show good agreement with the empirical model.

In conclusion, semiconducting nanowires of Sb-doped SnO_2 were successfully synthesized by co-evaporating Sn and Sb powders at 900 °C in an atmosphere composed of 1% oxygen and 99% nitrogen. Electrical investigations suggested that the resistance of the nanowire films would decrease by more than three orders of magnitude when Sb was doped into SnO_2 nanowires, which is of great significance for gas sensor fabrication and application. Our test results also indicated that Sb-doped SnO_2 nanowires showed a very short recovery time of about 5 s to 10 ppm ethanol gas at 300 °C. So Sb-doped SnO_2 nanowires will find a promising application for the fabrication of gas sensors with low resistance, and quick response and recovery times.

This work was supported by the project of Shanghai natural science fund (04JC 14080)

Notes and references

1 A. E. Rakhshani, Y. Makdisi and H. Ramazaniyan, *J. Appl. Phys.*, 1998, **83**, 1049–1057.
2 S. R. Dhage and V. Ravi, *Appl. Phys. Lett.*, 2003, **83**, 4539–4541.
3 A. Forleo, S. Capone, M. Epifani, P. Siciliano and R. Rella, *Appl. Phys. Lett.*, 2004, **84**, 744–746.
4 J. E. Dominguez, L. Fu and X. Q. Pan, *Appl. Phys. Lett.*, 2002, **81**, 5168–5170.
5 Y. Idota, T. Kubota, A. Matsufuji, Y. Maekawa and T. Miyasaka, *Science*, 1997, **276**, 1395–1397.
6 H. Kim and A. Piqué, *Appl. Phys. Lett.*, 2004, **84**, 218–220.
7 I. M. Chan, T. Y. Hus and F. C. Hong, *Appl. Phys. Lett.*, 2002, **81**, 1899–1901.
8 Z. Pan, Z. Dai and Z. L. Wang, *Science*, 2001, **291**, 1947–1949.
9 Z. Q. Liu, D. H. Zhang, S. Han, C. Li, T. Tang, W. Jin, X. L. Liu, B. Lei and C. W. Zhou, *Adv. Mater.*, 2003, **15**, 1754–1757.
10 D. F. Zhang, L. D. Sun, J. L. Yin and C. H. Yan, *Adv. Mater.*, 2003, **15**, 1022–1025.
11 Tao Gao and Taihong Wang, *Chem. Commun.*, 2004, 2558–2559.
12 P. Nguyen, H. T. Ng, J. Kong, A. M. Cassell, R. Quinn, J. Li, J. Han, M. McNeil and M. Meyyappan, *Nano Lett.*, 2003, **3**, 925–928.
13 S. H. Luo, Q. Wan, W. L. Liu, M. Zhang, Z. F. Di, S. Y. Wang, Z. T. Song, C. L. Lin and J. Y. Dai, *Nanotechnology*, 2004, **15**, 1424–1427.
14 Q. Wan, C. L. Lin, X. B. Yu and T. H. Wang, *Appl. Phys. Lett.*, 2004, **84**, 124–126.
15 E. Comini, G. Faglia, G. Sberveglieri, Z. Pan and Z. L. Wang, *Appl. Phys. Lett.*, 2002, **81**, 1869–1871.
16 R. W. J. Scott, S. M. Yang, G. Chabanis, N. Coombs, D. E. Williams and G. A. Ozin, *Adv. Mater.*, 2001, **13**, 1468–1472.